

# HER3 Targeting Sensitizes HNSCC to Cetuximab by Reducing HER3 Activity and HER2/HER3 Dimerization: Evidence from Cell Line and Patient-Derived Xenograft Models

Dongsheng Wang<sup>1</sup>, Guoqing Qian<sup>1</sup>, Hongzheng Zhang<sup>1</sup>, Kelly R. Magliocca<sup>2</sup>, Sreenivas Nannapaneni<sup>1</sup>, A.R.M. Ruhul Amin<sup>1</sup>, Michael Rossi<sup>3</sup>, Mihir Patel<sup>4</sup>, Mark El-Deiry<sup>4</sup>, J. Trad Wadsworth<sup>4</sup>, Zhengjia Chen<sup>5</sup>, Fadlo R. Khuri<sup>1</sup>, Dong M. Shin<sup>1</sup>, Nabil F. Saba<sup>1</sup>, and Zhuo G. Chen<sup>1</sup>

## Abstract

**Purpose:** Our previous work suggested that HER3 inhibition sensitizes head and neck squamous cell carcinoma (HNSCC) to EGFR inhibition with cetuximab. This study aimed to define the role of HER3 in cetuximab resistance and the antitumor mechanisms of EGFR/HER3 dual targeting in HNSCC.

**Experimental Design:** We treated cetuximab-resistant HNSCC UMSCC1-C and parental UMSCC1-P cell lines with anti-EGFR antibody cetuximab, anti-HER3 antibody MM-121, and their combination. We assessed activities of HER2, HER3, and downstream signaling pathways by Western blotting and cell growth by sulforhodamine B (SRB) and colony formation assays. HER3-specific shRNA was used to confirm the role of HER3 in cetuximab response. The combined efficacy and alterations in biomarkers were evaluated in UMSCC1-C xenograft and patient-derived xenograft (PDX) models.

**Results:** Cetuximab treatment induced HER3 activation and HER2/HER3 dimerization in HNSCC cell lines. Combined treat-

ment with cetuximab and MM-121 blocked EGFR and HER3 activities and inhibited the PI3K/AKT and ERK signaling pathways and HNSCC cell growth more effectively than each antibody alone. HER3 knockdown reduced HER2 activation and resensitized cells to cetuximab. Cetuximab-resistant xenografts and PDX models revealed greater efficacy of dual EGFR and HER3 inhibition compared with single antibodies. In PDX tissue samples, cetuximab induced HER3 expression and MM-121 reduced AKT activity.

**Conclusions:** Clinically relevant PDX models demonstrate that dual targeting of EGFR and HER3 is superior to EGFR targeting alone in HNSCC. Our study illustrates the upregulation of HER3 by cetuximab as one mechanism underlying resistance to EGFR inhibition in HNSCC, supporting further clinical investigations using multiple targeting strategies in patients who have failed cetuximab-based therapy. *Clin Cancer Res*; 23(3); 677–86. ©2016 AACR.

## Introduction

Targeting epidermal growth factor receptor (EGFR) in head and neck squamous cell carcinoma (HNSCC) is an attractive and

rational strategy given that more than 90% of these tumors overexpress EGFR (1, 2). Cetuximab, a chimerized antibody against EGFR, remains the only FDA-approved targeted agent for HNSCC since its approval in 2006. The addition of cetuximab to platinum and fluorouracil treatment resulted in improved overall survival of patients with recurrent/metastatic HNSCC, and this combination has been adopted as the current standard of care for this population (3). Despite this success, the overall response rate to cetuximab as a single agent does not exceed 13%, with a response duration of less than 2 to 3 months (4). Moreover, intrinsic and acquired resistance during EGFR therapy inevitably occurs (5, 6). Several mechanisms have been identified through which resistance to EGFR-targeted agents occurs in HNSCC. EGFR gene mutation and compensatory signaling from HER3 and other EGFR (ErbB) family members have been suggested to be associated with sensitivity to cetuximab therapy in HNSCC (7, 8).

HER3 (ErbB3) is a member of the human EGFR family, which consists of four type 1 transmembrane tyrosine kinase receptors: HER1 (EGFR, ErbB1), HER2 (Neu, ErbB2), HER3 (ErbB3), and HER4 (ErbB4). Upregulation of HER3 is commonly observed in various malignancies, including breast, colorectal carcinoma, HNSCC, gastric, ovarian, prostate, and bladder cancers, and

<sup>1</sup>Department of Hematology and Medical Oncology, Winship Cancer Institute at Emory, University School of Medicine, Atlanta, Georgia. <sup>2</sup>Department of Pathology, Emory University, Atlanta, Georgia. <sup>3</sup>Department of Radiation Oncology Emory University, Atlanta, Georgia. <sup>4</sup>Department of Otolaryngology Emory University, Atlanta, Georgia. <sup>5</sup>Department of Biostatistics and Bioinformatics, Emory School of Public Health, Emory, University, Atlanta, Georgia.

**Note:** Supplementary data for this article are available at Clinical Cancer Research Online (<http://clincancerres.aacrjournals.org/>).

**Corresponding Authors:** Zhuo G. Chen, Department of Hematology and Medical Oncology, Winship Cancer Institute, Emory University School of Medicine, 1365-C Clifton Road, Suite C3086, Atlanta, GA 30322. Phone: 404-778-3977; Fax: 404-778-5520; E-mail: gzchen@emory.edu; and Nabil F. Saba, Department of Hematology and Medical Oncology, Winship Cancer Institute, Emory University School of Medicine, 1365-C Clifton Road, Suite C3086, Atlanta, GA 30322. Phone: 404-778-1900; Fax: 404-686-4330; E-mail: NFSABA@emory.edu

**doi:** 10.1158/1078-0432.CCR-16-0558

©2016 American Association for Cancer Research.

### Translational Relevance

The clinical benefit of anti-EGFR therapy using cetuximab in head and neck squamous cell carcinoma (HNSCC) is limited by *de novo* or acquired resistance. Novel strategies to overcome this resistance are therefore highly justified. Activation of HER3 has previously been reported to negatively correlate with response to anti-EGFR therapy. In this study, we demonstrated that dual targeting of EGFR and HER3 was superior to EGFR targeting alone in clinically relevant HNSCC PDX models; both a cetuximab resistant cell line and PDX models consistently demonstrated upregulation of HER3 and HER2/HER3 dimer by cetuximab as one mechanism underlying resistance to EGFR inhibition in HNSCC. Our results support further clinical investigations using multiple targeting strategies in patients who have failed cetuximab-based therapy.

correlates with poorer survival (9–13). Upon binding of HRG1, the physiological HER3 receptor ligand, HER3 dimerizes with other ErbB family members, preferentially HER2. Dimerization results in transphosphorylation of HER3 on tyrosine residues contained within the cytoplasmic tail of the protein (14–16). Phosphorylation of these sites creates SH2 docking sites for SH2-containing proteins, and specifically PI3K (17). HER3 is a potent activator of AKT as it possesses six tyrosine phosphorylation sites with YXXM motifs that serve as excellent binding sites of the p85 regulatory subunit of PI3K, resulting in subsequent activation of the downstream AKT pathway (18, 19). These six PI3K sites serve as a strong amplifier of HER3 signaling. Activation of this pathway further elicits several important biological processes, including cell growth and survival (20). Ligand-independent HER2/HER3 interaction has also been reported in HER2-amplified cells (21). Because HER3 can dimerize with EGFR, HER2 even c-Met, it likely plays a central role in response to EGFR-targeted therapy. Identifying biomarkers that can predict the clinical activity of HER3 and EGFR-targeted therapy will be crucial in understanding the mechanism of resistance to anti-EGFR therapy in HNSCC.

This study aimed to elucidate the role of HER3 in cetuximab resistance in HNSCC, to investigate whether adding anti-HER3 treatment to cetuximab-based regimens can improve the treatment of HNSCC in models more relevant to the clinic, and to understand the underlying antitumor mechanisms of anti-EGFR/HER3 approaches. For that purpose, we addressed the role of HER3 in cetuximab resistance in three settings: HNSCC cell lines, a xenograft mouse model using a cetuximab-resistant HNSCC cell line, and multiple patient-derived xenograft (PDX) mouse models using tissues from HNSCC patients.

## Materials and Methods

### Cell lines and reagents

Cetuximab was obtained from ImClone, and MM-121/SAR256212 was provided by Merrimack Pharmaceuticals and Sanofi. Human HNSCC cell line UMSCC1-P and its cetuximab resistant counterpart UMSCC1-C were provided by Dr. Paul Harari (University of Wisconsin School of Medicine and Public Health, Madison, WI). The genotypes of the two cell lines were confirmed using the STR method by the Emory Integrated Genomics Core. The genotype of these two cell lines is identical to the

original UMSCC1 cell line published previously by Zhao and colleagues (22). All cell lines were maintained in Dulbecco's Modified Eagle's Media (DMEM) with 5% FBS and 0.4 µg/mL hydrocortisone at 37°C, 10% CO<sub>2</sub> (23).

### Colony formation assay

Cells were plated in 6-well culture plates at the concentration of 200 per well. After 24-hour incubation, cells were treated with PBS, cetuximab, MM-121, or the combination of cetuximab and MM-121 (CM combination) for 10 days to form colonies as previously described (24). Medium was changed every 3 days. The colonies were then stained with 0.2% crystal violet with buffered formalin (Sigma). Colony numbers were manually counted using ImageJ software. Cell numbers  $\geq 50$  were considered as a colony.

### Sulforhodamine B (SRB) assay

The SRB assay was used for cell growth determination. Cells were seeded in 96-well plates in medium containing PBS control, cetuximab, MM-121, and CM combination for 48 hours. Cells were fixed with 10% trichloroacetic acid (Sigma-Aldrich) after an additional 24 and 48 hours of culture. Cells then were washed 5 times with distilled and de-ionized water. After air drying, cells were incubated in 50 µL SRB (Sigma-Aldrich) for 10 minutes. Cells were then washed with 1% acetic acid 5 times. After air drying, 10 mmol/L Tris solution (pH 10) was added to dissolve the bound dye. Cell growth was assessed by optical density (OD) determination at 510 nm using a microplate reader.

### Western blot analysis

Lysates of cell lines and xenograft tissues were generated using lysis buffer as previously reported (25). The lysate was centrifuged at 16,000 × g at 4°C for 15 minutes. Total protein (40 µg) for each sample was separated by 8% to 10% SDS-PAGE and transferred onto a Westran S membrane (Whatman Inc.). Desired proteins were probed with corresponding antibodies. Rabbit anti-human AKT, ERK, pAKT, pERK, EGFR, pEGFR, HER2 pHER2, HER3, and pHER3 antibodies (1:1,000 dilutions) were purchased from Cell Signaling Technology, mouse anti-human β-actin (1:10,000 dilution) from Sigma, anti-human EGFR and HER3 antibodies from Santa Cruz Biotechnology, and anti-human pEGFR antibody from Millipore. HRP-conjugated secondary anti-mouse and anti-rabbit IgG (H+L) was obtained from Promega. Bound antibody was detected using the SuperSignal West Pico Chemoluminescence system (Pierce). ImageJ software was used for blot quantification. Protein densitometry was determined by ImageJ.

### HER3 knockdown

To knock down HER3 in UMSCC1-C cells, we used pLKO.1 puro vector (Addgene). Online software from www.ambion.com was used to locate three potential siRNA sequences. Three pairs of shRNA were designed following the protocol provided by lentiweb.com. Basically, three pairs of oligonucleotides each containing the shRNA sequence and hairpin sequence plus Age I and EcoR I sites were synthesized and cloned into the pLKO.1 lentiviral vector. Only one of the three constructed targeting sequences 'TGGTAGAGTAGAGAATTCATT' showed a significant knockdown effect after stable cell lines were made with puromycin selection. Western blot was carried out to confirm the HER3 knockdown efficiency in these purified cells. HER3 knockdown

cells were named UMSCC1-C/H cells. A vector control cell line, SCC1-C/pLKO1, was simultaneously generated.

#### Immunohistochemistry (IHC) staining and analysis

In brief, patient tumor tissues were harvested, fixed in 10% buffered formalin, and embedded in paraffin. The sections were incubated with a primary antibody: anti-EGFR (1:100 dilution; Cell Signaling Technology), anti-HER3 (1:100 dilution), followed by secondary antibody and diaminobenzidine (DAB, Vector Laboratories) staining. Nuclei were counterstained with hematoxylin OS (Vector Laboratories). Immunoglobulin G was used as a negative control. The quantifications were determined by at least two individuals blindly and independently. Briefly, the staining was scored for the proportion of stained tumor cells and for staining intensity; each on a four-point scale: 1: <5%, 2: 5%–20%, 3: 21%–50%, 4: 51%–100%, and 1 = no staining, 2 = low, 3 = moderate, and 4 = high, respectively. IHC scores = (proportion × intensity) as previously described (26). The highest score is 16. Scoring was done at 200× magnification.

#### Immunoprecipitation (IP)

Cells cultured in 10-cm dishes were collected and lysed with cold CHAP buffer with protease/phosphatase inhibitors. Total protein (2,000 µg) in 300 µL lysate buffer was incubated with anti-HER3 antibody (1:100) overnight at 4°C. Immunoprecipitation beads (50 µL; Pierce ProteinA/G Agarose, ThermoScientific) were directly dispensed into each lysate and further incubated for 2 hours. Immunoprecipitation beads were then spun down and washed three times with CHAP buffer. The pellet was then suspended in SDS-PAGE loading buffer.

#### In vivo xenograft treatment study

The animal experimental protocol was approved by the Institutional Animal Care and Use Committees of Emory University. In brief,  $2 \times 10^6$  UMSCC1-C1 cells were injected subcutaneously into nude mice (athymic nu/nu, Taconic, NY) ages 4 to 6 weeks. Mice were randomly divided into five groups after tumor formation: PBS control, cetuximab 100 µg/dose, MM-121 300 µg/dose (MM-121.LD), and combination with low dose of MM-121 (comb. LD) and combination with high dose of MM-121 600 µg/dose (comb. HD;  $n = 7$  for each treatment group). Doses were chosen based on previous studies (24, 27). Drugs were given by intraperitoneal (i.p.) injection twice a week. Tumor volume and body weight were measured three times a week. Tumor volume was calculated using the formula:  $V = \pi/6 \times \text{larger diameter} \times (\text{smaller diameter})^2$ , as reported previously (28).

#### PDX animal models

Briefly, fresh tumor tissue from patients with HNSCC consented at the Midtown Hospital, Emory University (Atlanta, GA) in accordance with the protocol approved by the Emory Institutional Review Board was collected. Tumor section was cut into 3 mm × 3 mm × 3 mm small pieces, which were then implanted into the hind flanks of NOD SCID mice (Charles River Laboratories International, Inc). Upon reaching 1,500 mm<sup>3</sup>, tumors were passed to a second colony of athymic nu/nu nude mice (Harlan). The third generation of 24 nude mice was divided into 4 groups for drug treatment: PBS control, cetuximab 100 µg/dose, MM-121 300 µg/dose (MM-121.LD), and combination with low dose of MM-121 (comb. LD).

#### Statistical analysis

Comparison of means from multiple treatment groups was carried out using one-way ANOVA or Kruskal–Wallis test to determine the significance of tumor growth inhibition among treatment groups. A Bonferroni correction was introduced to correct for multiple comparisons. The pairwise comparison was used to compare mean tumor volumes of cell growth inhibition between the different groups over time. All *P* values were two-sided and *P* values less than 0.05 were considered statistically significant.

## Results

#### Cetuximab induces HER3 expression and activation in HNSCC cell lines

The compensatory overexpression of other HER family members has been implicated as one of the mechanisms that drive cetuximab resistance (7). To determine whether HER3 expression is affected by cetuximab, we treated both the cetuximab-resistant UMSCC1-C cell line and its sensitive parental cell line UMSCC1-P with cetuximab. Ligand binding of HER3 causes a change in conformation that allows for dimerization, phosphorylation, and activation of HER3. Phosphorylation of HER3 at specific sites such as Y1289 and Y1222 by its heterodimerization partner, such as HER2, implicates activation of this protein. As shown in Fig. 1A and B, both HER3 expression and activation (indicated by the level of pHER3) were elevated in a time-dependent manner. Induction and activation of HER3 by cetuximab was stronger in UMSCC1-C cells than in UMSCC1-P cells.

#### HER2/HER3 dimerization is increased upon cetuximab treatment in UMSCC1-C cells

HER2/HER3 heterodimerization plays an important role in cancer progression (29–31). To examine whether cetuximab treatment has any effect on HER2/HER3 dimerization, we conducted an IP study. UMSCC1-C cells were incubated in the indicated cell medium with 5% FBS and 2 µg/mL cetuximab for 24 hours. HER3 was immunoprecipitated with anti-HER3 antibody from the cell lysate. The immunoprecipitate was fractionated on SDS-PAGE followed by immunoblotting with anti HER2 and HER3. As Fig. 2 shows, cetuximab treatment increased not only HER3 expression but also HER2 and HER3 association in UMSCC1-C cells, as illustrated by the greater level of HER2 detected in immunoblot analysis. The increase in HER2/HER3 dimerization by cetuximab treatment was also observed in MDA686TU cells (Supplementary Fig. S1).

#### Inhibition of HER3 resensitizes resistant cell line UMSCC1-C to cetuximab

To determine if the reduction of HER3 expression has any effect on cetuximab sensitivity of the resistant cell line UMSCC1-C, we knocked down HER3 in UMSCC1-C cells with the pLKO.1 system to generate a stable cell line, UMSCC1-C/H, in which HER3 expression was reduced by more than 85% (Fig. 3A). Interestingly, as HER3 level was knocked down, the levels of activated HER2 (pHER2) and AKT (pAKT) were also largely reduced as compared with the control UMSCC1-C cells (Fig. 3A). SRB assay was performed to determine the sensitivity to cetuximab in parental UMSCC1-P, UMSCC1-C, and HER3 knockdown UMSCC1-C/H cells. As shown in Fig. 3B, the sensitivity of UMSCC1-C/H cells to cetuximab was recovered. Our previous study indicated a

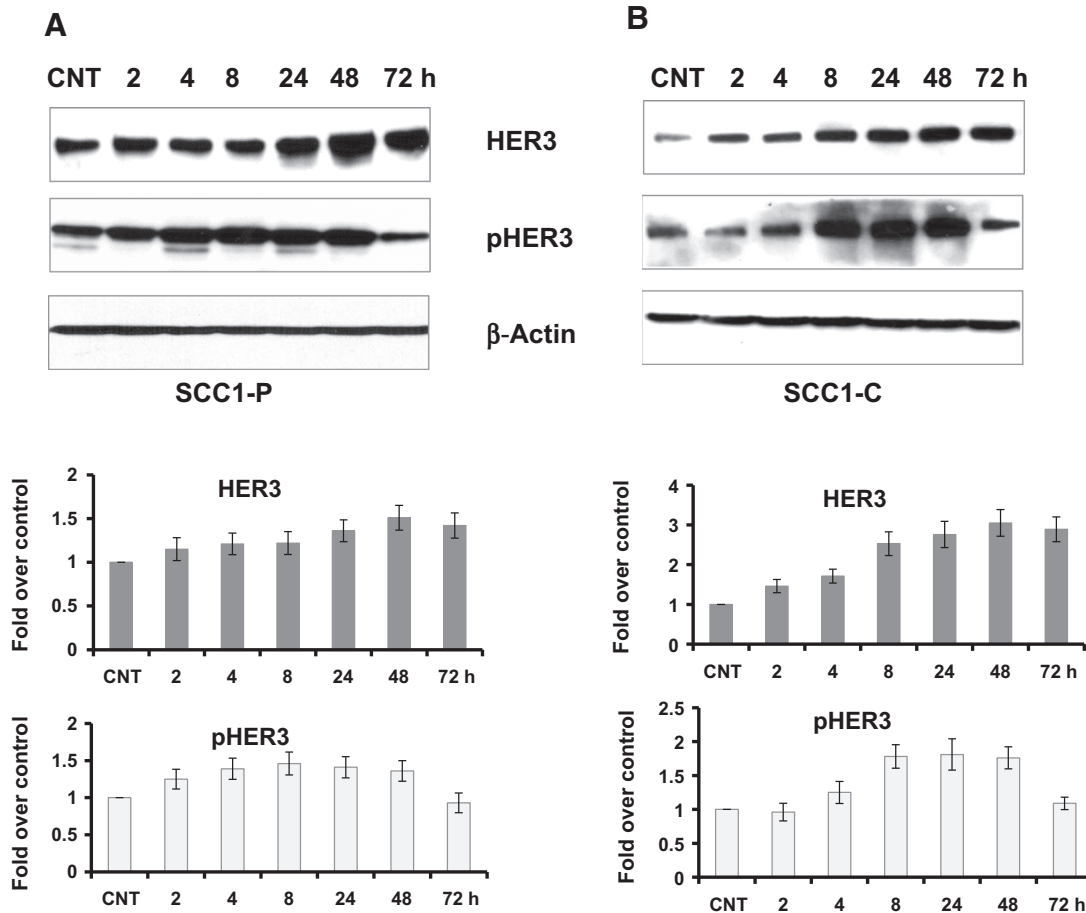


**Figure 1.** Cetuximab induces HER3 expression and activation in HNSCC cell lines. Cetuximab-sensitive UMSSC1-P cells (A) and counterpart resistant UMSSC1-C cells (B) were cultured in medium with 5% FBS. The cells were treated with 2 µg/mL cetuximab for the indicated times. CNT indicates the control sample. Both HER3 expression and activation (pHER3) levels were elevated by cetuximab treatment in a time-dependent manner (the figure represents 1 of 3 experiments). The average fold increase was determined from 3 individual experiments with standard deviations.

synergistic inhibitory effect of cetuximab and MM-121 on HNSCC cell lines TU212 and UMSSC47. In this study, SRB assay and colony formation assay were carried out to compare the growth-inhibitory effect of MM-121 and its combination with cetuximab in UMSSC1-P, UMSSC1-C, and UMSSC1-C/H cells. In UMSSC1-C cells, treatment with cetuximab alone did not inhibit cell growth. However, MM-121 resensitized UMSSC1-C to cetuximab, as shown by the significant inhibition of cell growth by the combined treatment (Fig. 3C). The MM-121 and cetuximab combination showed significantly greater inhibition of colony formation in comparison with either single drug in all three cell lines (Fig. 3D). Consistent with the observations using the SRB assay, knockdown of HER3 in UMSSC1-C/H cells restored cell sensitivity to cetuximab, as indicated by the significant reduction in colony number in UMSSC1-C/H cells when treated with cetuximab as compared with UMSSC1-C cells (Fig. 3D).

**Combination of cetuximab and MM-121 inhibits both PI3K/AKT and ERK signaling pathways**

HER family receptors activate a number of important signal transduction pathways, including PI3K/AKT and ERK pathways,

which are critical for cell growth. To identify the mechanism underlying the restoration of cetuximab sensitivity in the resistant cells, we treated both UMSSC1-P and UMSSC1-C cells with cetuximab, MM-121, and the combination and conducted a Western blot assay to determine alterations in the PI3K/AKT and ERK pathways resulting from cetuximab and MM-121 treatment. As shown in Fig. 4, the combination of cetuximab and MM-121 more potently inhibited both ERK and AKT pathways compared with each single agent. Inhibition of HER3 by MM-121 affected mainly the pAKT level while only moderate ERK alteration was observed.

**Inhibition of HER3 resensitizes resistant HNSCC tumor to cetuximab in xenograft models**

To expand our findings into the *in vivo* setting, a xenograft model using the cetuximab-resistant UMSSC1-C cell line in nude mice was established as previously described (7, 24). Mice were randomly assigned to five treatment groups: PBS control, cetuximab (C), MM-121 (M), and combination of cetuximab and MM-121 (CM high and low). Mice were treated twice a week through i.p. injection. Consistent with our *in vitro* observations, the CM

Downloaded from http://aacrjournals.org/clinccancerres/article-pdf/23/3/677/2043423/677.pdf by guest on 23 May 2025

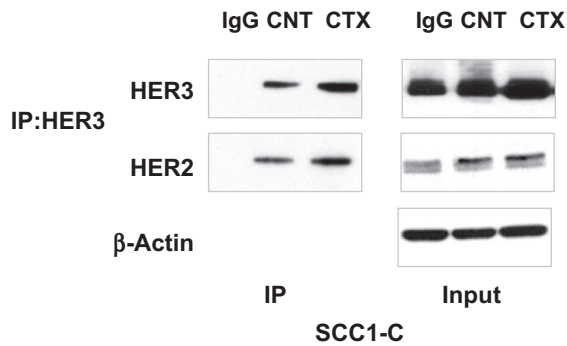


**Figure 2.**

HER2/HER3 dimerization is increased upon cetuximab treatment. UMSCC1-C cells were exposed to 2  $\mu\text{g}/\text{mL}$  cetuximab for 24 hours. HER3 was immunoprecipitated from the cell lysate with anti-HER3 antibody. The immunoprecipitate was fractionated on SDS-PAGE followed by immunoblotting with anti-HER2 and HER3 antibodies. As the image shows, cetuximab treatment increased HER3 expression in UMSCC1-C cells, and at the same time HER2 and HER3 association was increased as more HER2 was detected by immunoblot in cetuximab-treated cells compared with control cells and IgG control.  $\beta$ -Actin was used as a loading control (the figure represents 1 of 3 experiments).

combination showed the greatest tumor growth inhibition of UMSCC1-C xenografts. As shown in the tumor volume measurement in Fig. 5A, neither cetuximab nor MM-121 significantly reduced tumor growth compared with the PBS control. However, the group treated with CM combination showed significantly suppressed tumor growth as compared with the PBS control ( $P < 0.001$ ), cetuximab ( $P < 0.001$ ), and MM-121 ( $P < 0.001$ ) alone for both high- and low-dose combination. Furthermore, in UMSCC1-C/H cells where HER3 expression is knocked down, the xenografted tumor was resensitized to cetuximab, such that cetuximab alone was sufficient to significantly inhibit UMSCC1-C/H tumor growth as compared with the control (Fig. 5B;  $P < 0.001$ ).

#### Combination of MM-121 and cetuximab shows strong antitumor activity in multiple PDX models

Tumor tissues from 6 patients with HNSCC were used to generate PDX models. The clinical characteristics of each patient are shown in Supplementary Table S1. EGFR and HER3 expression levels in each patient tumor sample are shown in Supplementary Figure S2A and S2B. For each PDX model, 6 tumor bearing mice were randomly assigned to each group treated with PBS, cetuximab (100  $\mu\text{g}/\text{dose}$ ), MM-121 (300  $\mu\text{g}/\text{dose}$ ), and the combination (100  $\mu\text{g}/\text{dose}$  cetuximab/300  $\mu\text{g}/\text{dose}$  MM-121). In PDX models derived from patient 1 (FOM/tongue), patient 2 (pyriform), patient 4 (larynx, recurrent tumor with prior cetuximab treated), and patient 5 (retromolar trigone), both cetuximab and the combination significantly inhibited tumor growth in nude mice ( $P < 0.001$  for both treatment; Fig. 6A; Supplementary Figure S3A–S3C; Table S1). There was no significant difference in tumor growth inhibition between single cetuximab and the combination treatment. However, the PDX tumors derived from patient 1 grew back after stopping the treatment with cetuximab alone, while no tumor relapse was detected in the combination group (Fig. 6A). Moreover, only the combined treatment could

completely block the tumors growth in most of the mice even in recurrent patient (patient 4) PDX (Supplementary Fig. S3). In PDX models derived from patient 8 (supraglottis), only the combination treatment significantly inhibited tumor growth ( $P < 0.004$ ; Fig. 6B). We have identified a KRAS mutation by RNA-seq in this patient sample (data not shown). The combined treatment was also more effective than either single agent ( $P < 0.032$  and  $P < 0.035$ , respectively). In PDX models derived from patient 3 (FOM), both cetuximab and the combination significantly inhibited tumor growth in nude mice ( $P < 0.001$  for both treatment; Supplementary Figs. S4A and S4B). However, the combination was significantly more effective than either of the single agents ( $P < 0.01$  for both). Interestingly, Western blot analyses of PDX tissues from patients 3 and 8 indicated induction of HER3 expression by cetuximab and reduction of AKT activity by MM-121 (Fig. 6C). This is consistent with our observations in *in vitro* cell lines.

## Discussion

The clinical benefit of anti-EGFR therapy in HNSCC is limited by *de novo* and acquired resistance. Novel strategies to overcome this resistance are therefore highly justified. The HER3 protein is reportedly expressed in 32% to 87% HNSCC patient tumors (depending on the study) and is positively correlated with invasion and metastasis (32–34). Hyperactivation of HER3 has previously been reported to negatively correlate with response to anti-EGFR therapy (35). Moreover, HER3 activation represents a critical step by which HNSCC cells escape from cetuximab inhibition (7). Dual inhibition of both EGFR and HER3 is hence an attractive clinical strategy for treating HNSCC. Harari's group observed a strong activation of HER3 in established cetuximab-resistant cell lines. They also found that MEHD7945A, a monoclonal antibody that targets both EGFR and HER3, was more effective than a combination of cetuximab and anti-HER3 antibody at inhibiting both EGFR/HER3 signaling and tumor growth (36). Nakagawa and colleagues have shown that the HER3 ligand heregulin is associated with both *de novo* and acquired resistance to cetuximab (37). They also found that patritumab, an antibody specific for HER3, is able to overcome such resistance. Our recent research identified that high heregulin mRNA and high HER3 protein levels are independent prognostic factors for poor overall survival in patients with oropharyngeal squamous cell carcinoma (OPSCC; ref. 38). Our current study further demonstrated both *in vitro* and *in vivo* that inhibiting HER3 could resensitize cetuximab-resistant HNSCC cells to this agent.

In addition, we have previously shown that the combination of cetuximab and MM-121 significantly inhibited HNSCC tumor cell growth both *in vitro* and *in vivo* through inhibition of AKT, ERK, and S6 signaling pathways, suggesting that a multitargeting approach to the EGFR family of signaling receptors may provide potential clinical benefit for patients with HNSCC (24). In the current study, we demonstrated that HER3 expression and activity is upregulated after cetuximab treatment, suggesting that HER3 may hold the key to cetuximab resistance. Previous studies have shown that HER3 activity plays an important role in AKT activation (15, 39) and is induced by cetuximab, possibly due to the inhibition of AKT activity, which in turn induces HER3 expression through FOXO

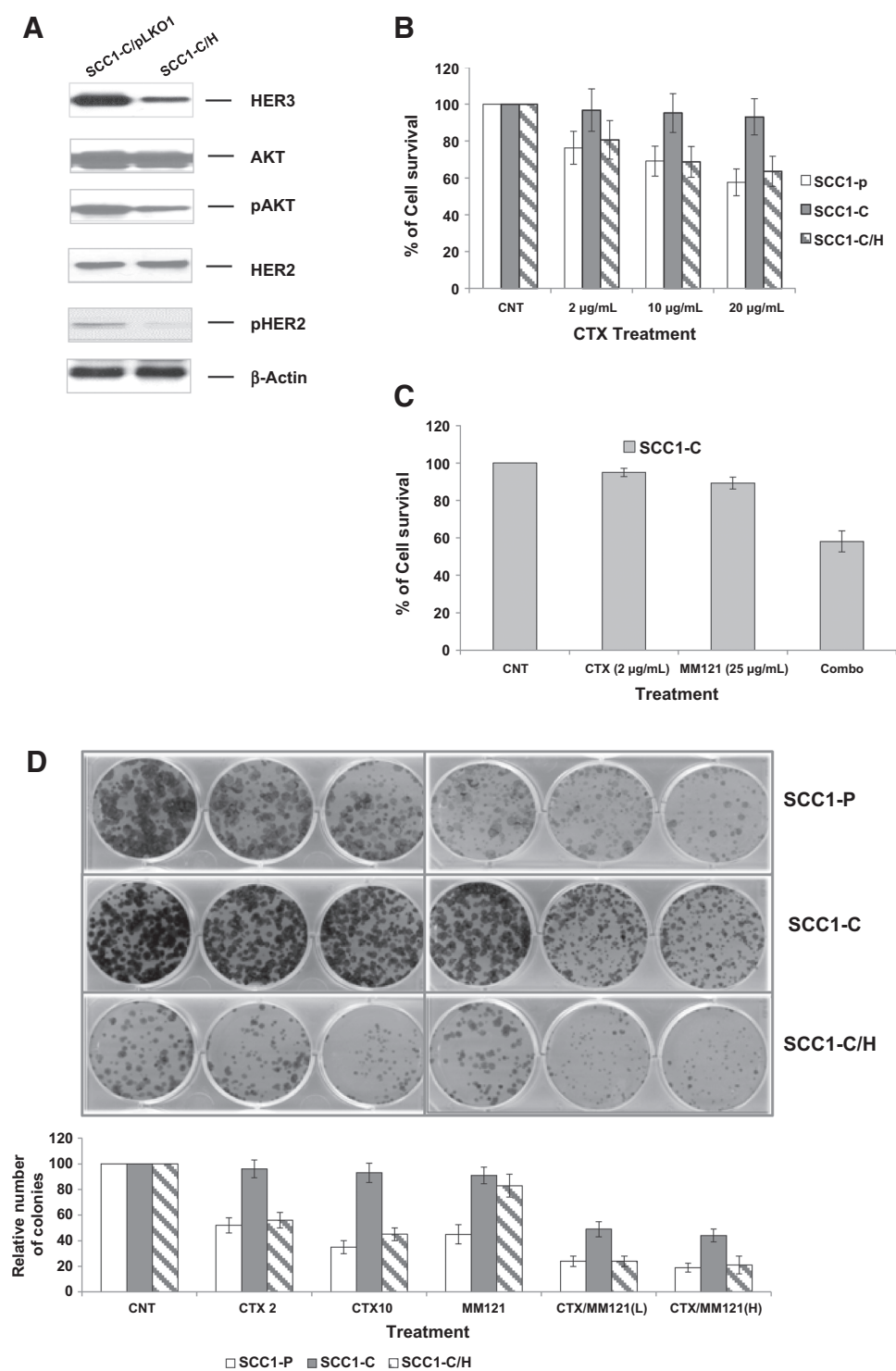


**Figure 3.** Inhibition of HER3 resensitizes the resistant UMSSCC1-C cell line to cetuximab. **A**, HER was knocked down in UMSSCC1-C/H cells. HER2 and AKT activities were also reduced, as demonstrated by a decrease in both pHER2 and pAKT levels. **B**, SRB assay shows that cetuximab reduces the growth rate of sensitive parental UMSSCC1-P cells at the indicated concentrations after treatment for 48 hours. No growth inhibition was observed in UMSSCC1-C cells. Knock down of HER3 by shRNA resensitized UMSSCC1-C cells to cetuximab inhibition. **C**, Combination of cetuximab (2 μg/mL) and MM-121 (25 μg/mL) (combo) more potently inhibited UMSSCC1-C growth in SRB assay. **D**, In a colony formation assay, cetuximab inhibited colony formation of UMSSCC1-P cells but not of UMSSCC1-C cells at the indicated concentration. When HER3 was knocked down by shRNA, cetuximab inhibition of colony formation was restored. Inhibition of HER3 by its antibody MM-121 (25 μg/mL) also resensitized UMSSCC1-C to cetuximab treatment. (CTX2: cetuximab 2 μg/mL, CTX10: cetuximab 10 μg/mL, CTX/MM-121 (L): combination of cetuximab 2 μg/mL and MM-121, CTX/MM-121 (H): combination of cetuximab 10 μg/mL and MM-121). Image represents 3 individual experiments.

(40). The inhibitory effect of cetuximab on AKT activation is, however, reduced as the elevated HER3 activates AKT, which prevents its complete inhibition. Our data demonstrated that either the combination of cetuximab and MM-121 or the use of shRNA against HER3 more potently reduced AKT activity and exerted greater cell growth inhibition in cetuximab-resistant

cells than cetuximab alone, which is consistent with the findings from other groups (7, 41). More importantly, knockdown of HER3 with shRNA resulted in reduction of activated HER2, suggesting that HER2/HER3 heterodimerization probably contributes to cetuximab resistance. This notion is supported by our immunoprecipitation results demonstrating an increase in

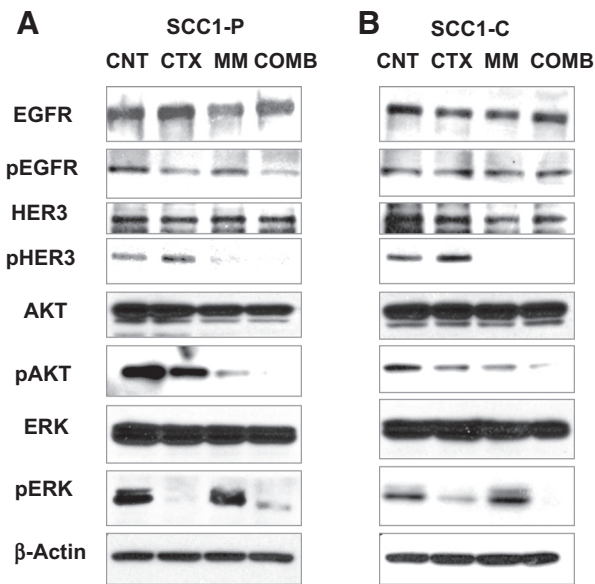


**Figure 4.** Combination of cetuximab and MM-121 inhibits both PI3K/AKT and ERK signaling pathways. UMSSC1-P (**A**) and UMSSC1-C (**B**) cells were treated with 2  $\mu\text{g}/\text{mL}$  cetuximab, 125  $\mu\text{g}/\text{mL}$  MM-121, and the combination, respectively. As shown in **A** and **B**, after 48 hours of treatment, AKT and ERK activation was simultaneously ablated by the combination compared to single drugs and the control. The inhibition of pAKT was greater by MM-121 than cetuximab in both cell lines (the figure represents 1 of 3 experiments).

the HER3 expression level following cetuximab exposure with greater HER3/HER2 heterodimerization, which is consistent with previous studies demonstrating increased HER2/HER3 dimerization leading to the activation of both HER2 and HER3 and their downstream signaling pathway in cancer (29, 42).

Antibody-dependent cell-mediated cytotoxicity (ADCC) plays an important role in antibody-based cancer therapy. ADCC has been reported for cetuximab (43, 44). In our study, MM-121 itself cannot trigger ADCC, because of its IgG2 isotype (45). Although the influence of MM121 on cetuximab ADCC in nude mice is unknown, it is unlikely that ADCC is the main reason for the resensitization of the resistant cancer cell line to cetuximab. However, the effect of MM121 on ADCC of cetuximab deserves further investigation.

In our xenograft models using the cetuximab-resistant UMSSC1-C cell line, neither cetuximab nor MM-121 alone significantly reduced tumor growth compared with PBS. The combination group, however, had significantly suppressed tumor growth compared with the single-agent control. This result further supports the role of HER3 in cetuximab resistance. To our knowledge, this is the first study to explore dual inhibition of EGFR and HER3 in xenograft tumor models derived from patient-derived tumor tissue (PDTT). At low passage, it is believed that PDTT will conserve the original tumor characteristics, such as heterogeneous histology, clinical biomolecular signature, malignant phenotypes and genotypes, tumor architecture, and tumor vasculature (46–48). Patient-derived tumor grafts are believed to offer relevant predictive insights into clinical outcomes when evaluating the efficacy of novel cancer therapies. PDX models are biologically stable in

terms of global gene expression patterns, mutational status, metastatic potential, drug response, and tumor structure when passaged in short generations of mice. These characteristics might provide significant improvements over established cell-line xenograft models (49). We conducted PDX animal studies using tissues derived from 6 patients. Our study demonstrated the improved efficacy of the combination compared with single antibodies. Meanwhile immunoblotting from the available tumor samples revealed an elevated level of HER3 following cetuximab treatment, and a reduction in AKT activity following exposure to anti-HER3 *in vivo*. This further solidifies our *in vitro* observations. The lack of significant clinical activity using prior dual EGFR and HER inhibitors in HNSCC probably stems from the fact that these studies did not focus on a cetuximab-resistant population; we believe, based on our results, future clinical investigations ought to focus on patients with prior exposure to EGFR inhibitors and perhaps with a more specific biomarker profile.

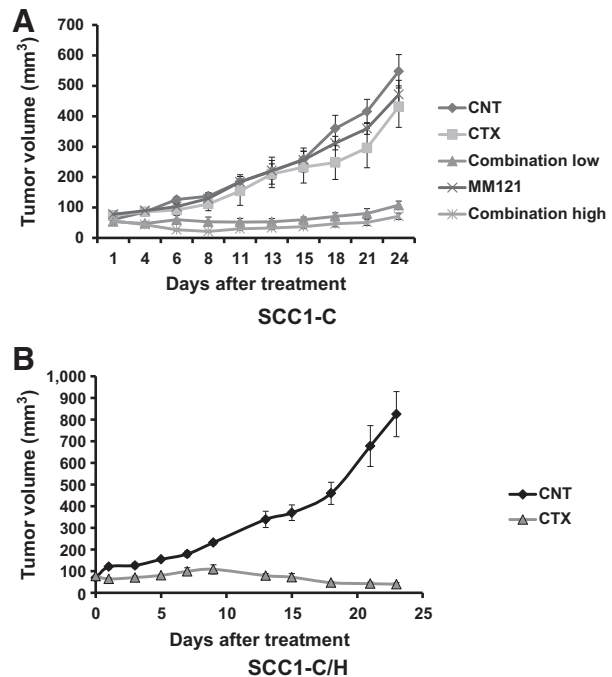


**Figure 5.** Combination of cetuximab and MM-121 shows strong antitumor activity in HNSCC cetuximab-resistant tumor xenograft animal model. **A**, In xenograft models using cetuximab-resistant UMSSC1-C cells, mice were randomly assigned to five treatment groups: PBS control, cetuximab (100  $\mu\text{g}/\text{dose}$ ), MM-121 (300  $\mu\text{g}/\text{dose}$ ), Comb.LD (cetuximab 100  $\mu\text{g}/\text{dose}/\text{MM-121}$  300  $\mu\text{g}/\text{dose}$ ), and Comb.HD (cetuximab 100  $\mu\text{g}/\text{dose}/\text{MM-121}$  600  $\mu\text{g}/\text{dose}$ ) and were treated twice a week through i.p. injection. Consistent with our *in vitro* observations, the CM combination showed the greatest tumor growth inhibition in UMSSC1-C xenografts. Neither cetuximab nor MM-121 alone significantly reduced the tumor growth compared with PBS control. However, the groups treated with both high and low doses of CM combination showed significantly suppressed tumor growth as compared with those treated with PBS control, cetuximab, and MM-121 alone ( $P < 0.001$ ,  $n = 6$ ). **B**, Mice carrying UMSSC1-C/H cell xenografts were randomly assigned to two treatment groups: PBS control, cetuximab (100  $\mu\text{g}/\text{dose}$ ). Treatment with cetuximab significantly inhibited tumor growth ( $P < 0.001$ ,  $n = 6$ ).

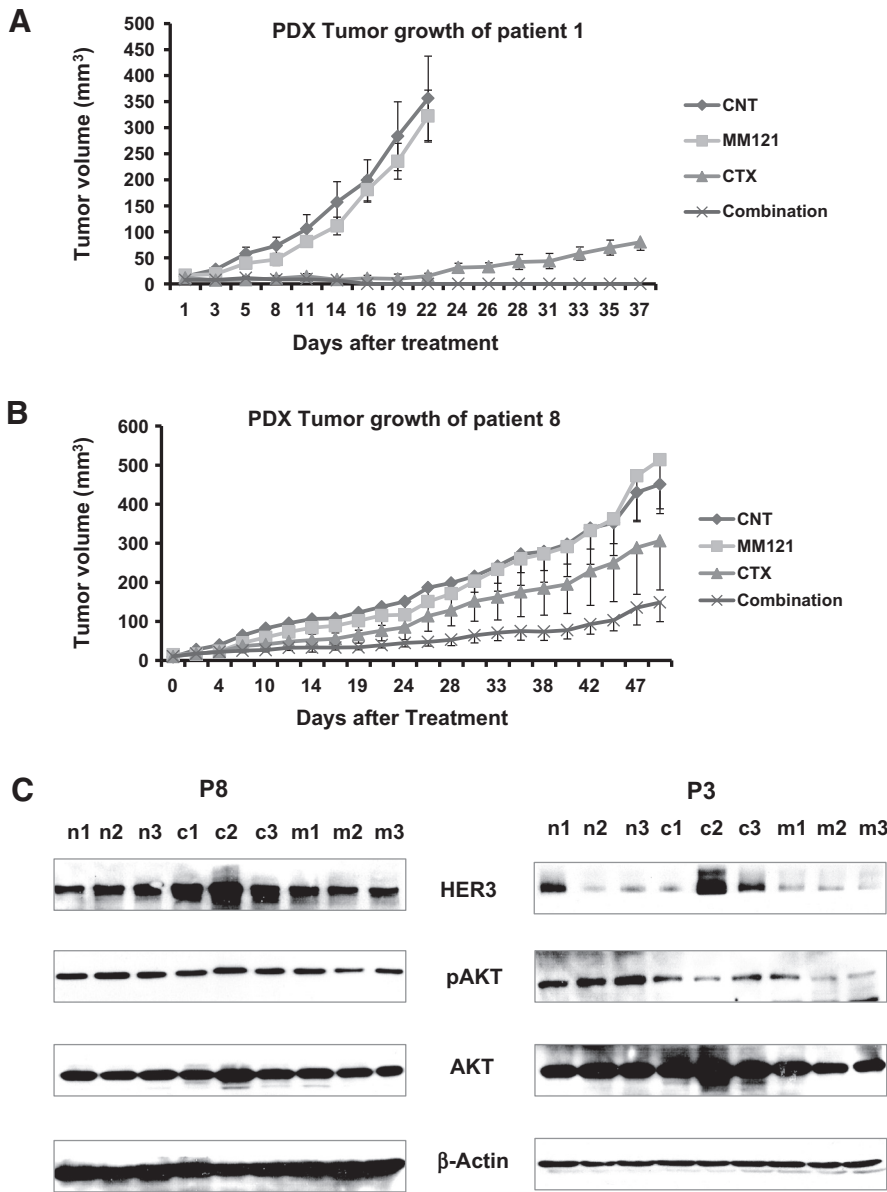


**Figure 6.**

Combination of anti-HER3 antibody MM-121 and cetuximab more potently inhibits tumor growth in HNSCC patient-derived tumor xenografts than single treatment with only MM-121 or cetuximab alone. **A**, In PDXs derived from patient 1 tumor tissue, both cetuximab (100 μg/dose) and the combination (cetuximab 100 μg/dose and MM-121 300 μg/dose) significantly inhibited tumor growth in nude mice ( $P < 0.001$  for both treatments). There was no significant difference between cetuximab alone and the combination. However, tumors treated with cetuximab alone grew back while no tumor relapse could be detected in the combination group. **B**, In PDXs derived from patient 8, only the combination treatment significantly inhibited tumor growth ( $P < 0.004$ ). Combination treatment was also more effective than either single agent ( $P < 0.032$  respectively). **C**, As shown by immunoblotting, HER3 expression was induced in cetuximab-treated PDX tumor samples, while pAKT was reduced by MM-121 treatment. No samples from the combination-treated PDXs were available for testing as the tumors were too small to isolate sufficient protein sample. n1-3: PDX tumor samples from 3 different PDXs in the control group. c1-3: three different tumor samples from the cetuximab-treated group. m1-3: three different tumor samples from the MM-121-treated group. Image represents 3 repeated experiments.

Taken together, our results demonstrate for the first time that dual targeting of EGFR and HER3 is more effective than EGFR targeting alone in HNSCC using a PDX model. Because this model is highly clinically predictive, our results pave the way for further clinical investigation focusing on pan-HER inhibition in a carefully selected HNSCC patient population, specifically those who have progressed after cetuximab-based therapy.

**Disclosure of Potential Conflicts of Interest**

M. Patel is a consultant/advisory board member for AstraZeneca and Intuitive Surgical. No potential conflicts of interest were disclosed by the other authors.

**Authors' Contributions**

Conception and design: A.R.M.R. Amin, Z. Chen, D.M. Shin, N.F. Saba, Z.G. Chen

Development of methodology: D. Wang, N.F. Saba, Z.G. Chen  
 Acquisition of data (provided animals, acquired and managed patients, provided facilities, etc.): D. Wang, G. Qian, H. Zhang, K.R. Magliocca, S. Nannapaneni, M. Rossi, M. Patel, M. El-Deiry, J.T. Wadsworth, Z.G. Chen  
 Analysis and interpretation of data (e.g., statistical analysis, biostatistics, computational analysis): G. Qian, S. Nannapaneni, A.R.M.R. Amin, M. Rossi, Z. Chen, F.R. Khuri, D.M. Shin, N.F. Saba, Z.G. Chen  
 Writing, review, and/or revision of the manuscript: D. Wang, G. Qian, K.R. Magliocca, A.R.M.R. Amin, M. Patel, M. El-Deiry, J.T. Wadsworth, Z. Chen, F.R. Khuri, D.M. Shin, N.F. Saba, Z.G. Chen  
 Administrative, technical, or material support (i.e., reporting or organizing data, constructing databases): H. Zhang, K.R. Magliocca, S. Nannapaneni, Z.G. Chen  
 Study supervision: M. El-Deiry, N.F. Saba, Z.G. Chen

**Acknowledgments**

The authors thank Dr. Anthea Hammond for her editing of the manuscript.

Downloaded from <http://aacrjournals.org/clinccancerres/article-pdf/23/3/677/2043423/677.pdf> by guest on 23 May 2025



## Grant Support

The present study was supported by grants from NIH (R21 CA182662, PIs N. F. Saba and Z.G. Chen) and WCI Gregory Family Fund to Drs. N.F. Saba and Z.G. Chen.

The costs of publication of this article were defrayed in part by the payment of page charges. This article must therefore be hereby marked

*advertisement* in accordance with 18 U.S.C. Section 1734 solely to indicate this fact.

Received March 3, 2016; revised May 30, 2016; accepted June 21, 2016; published OnlineFirst June 29, 2016.

## References

- Ongkeko WM, Altuna X, Weisman RA, Wang-Rodriguez J. Expression of protein tyrosine kinases in head and neck squamous cell carcinomas. *Am J Clin Pathol* 2005;124:71–6.
- Bei R, Budillon A, Masuelli L, Cereda V, Vitolo D, Di Gennaro E, et al. Frequent overexpression of multiple ErbB receptors by head and neck squamous cell carcinoma contrasts with rare antibody immunity in patients. *J Pathol* 2004;204:317–25.
- Vermorken JB, Mesia R, Rivera F, Remenar E, Kawecki A, Rottey S, et al. Platinum-based chemotherapy plus cetuximab in head and neck cancer. *N Engl J Med* 2008;359:1116–27.
- Vermorken JB, Trigo J, Hitt R, Koralewski P, Diaz-Rubio E, Rolland F, et al. Open-label, uncontrolled, multicenter phase II study to evaluate the efficacy and toxicity of cetuximab as a single agent in patients with recurrent and/or metastatic squamous cell carcinoma of the head and neck who failed to respond to platinum-based therapy. *J Clin Oncol* 2007;25:2171–7.
- Shaib W, Kono S, Saba N. Antiepidermal growth factor receptor therapy in squamous cell carcinoma of the head and neck. *J Oncol* 2012;2012:521215.
- Pao W, Miller VA, Politi KA, Riely GJ, Somwar R, Zakowski MF, et al. Acquired resistance of lung adenocarcinomas to gefitinib or erlotinib is associated with a second mutation in the EGFR kinase domain. *PLoS Med* 2005;2:e73.
- Wheeler DL, Huang S, Kruser TJ, Nechrebecki MM, Armstrong EA, Benavente S, et al. Mechanisms of acquired resistance to cetuximab: role of HER (ErbB) family members. *Oncogene* 2008;27:3944–56.
- Vlacich G, Coffey RJ. Resistance to EGFR-targeted therapy: a family affair. *Cancer Cell* 2011;20:423–5.
- Zhang J, Saba NF, Chen GZ, Shin DM. Targeting HER (ERBB) signaling in head and neck cancer: an essential update. *Mol Aspects Med* 2015;45:74–86.
- Slamon DJ, Clark GM. Amplification of c-erbB-2 and aggressive human breast tumors? *Science* 1988;240:1795–8.
- Maurer CA, Friess H, Kretschmann B, Zimmermann A, Stauffer A, Baer HU, et al. Increased expression of erbB3 in colorectal cancer is associated with concomitant increase in the level of erbB2. *Hum Pathol* 1998;29:771–7.
- Lee-Hoeflich ST, Crocker L, Yao E, Pham T, Munroe X, Hoeflich KP, et al. A central role for HER3 in HER2-amplified breast cancer: implications for targeted therapy. *Cancer Res* 2008;68:5878–87.
- Beji A, Horst D, Engel J, Kirchner T, Ullrich A. Toward the prognostic significance and therapeutic potential of HER3 receptor tyrosine kinase in human colon cancer. *Clin Cancer Res* 2012;18:956–68.
- Soltoff SP, Carraway KLIII, Prigent SA, Gullick WG, Cantley LC. ErbB3 is involved in activation of phosphatidylinositol 3-kinase by epidermal growth factor. *Mol Cell Biol* 1994;14:3550–8.
- Prigent SA, Gullick WJ. Identification of c-erbB-3 binding sites for phosphatidylinositol 3'-kinase and SHC using an EGF receptor/c-erbB-3 chimera. *EMBO J* 1994;13:2831–41.
- Fedi P, Pierce JH, di Fiore PP, Kraus MH. Efficient coupling with phosphatidylinositol 3-kinase, but not phospholipase C gamma or GTPase-activating protein, distinguishes ErbB-3 signaling from that of other ErbB/EGFR family members. *Mol Cell Biol* 1994;14:492–500.
- Zhang X, Gureasko J, Shen K, Cole PA, Kuriyan J. An allosteric mechanism for activation of the kinase domain of epidermal growth factor receptor. *Cell* 2006;125:1137–49.
- Suenaga A, Takada N, Hatakeyama M, Ichikawa M, Yu X, Tomii K, et al. Novel mechanism of interaction of p85 subunit of phosphatidylinositol 3-kinase and ErbB3 receptor-derived phosphotyrosyl peptides. *J Biol Chem* 2005;280:1321–6.
- Hynes NE, Lane HA. ERBB receptors and cancer: the complexity of targeted inhibitors. *Nat Rev Cancer* 2005;5:341–54.
- Sergina NV, Rausch M, Wang D, Blair J, Hann B, Shokat KM, et al. Escape from HER-family tyrosine kinase inhibitor therapy by the kinase-inactive HER3. *Nature* 2007;445:437–41.
- Junttila TT, Akita RW, Parsons K, Fields C, Lewis Phillips GD, Friedman LS, et al. Ligand-independent HER2/HER3/PI3K complex is disrupted by trastuzumab and is effectively inhibited by the PI3K inhibitor GDC-0941. *Cancer Cell* 2009;15:429–40.
- Zhao M, Sano D, Pickering CR, Jasser SA, Henderson YC, Clayman GL, et al. Assembly and initial characterization of a panel of 85 genomically validated cell lines from diverse head and neck tumor sites. *Clin Cancer Res* 2011;17:7248–64.
- Brenner JC, Graham MP, Kumar B, Saunders LM, Kupfer R, Lyons RH, et al. Genotyping of 73 UIM-SCC head and neck squamous cell carcinoma cell lines. *Head Neck* 2010;32:417–26.
- Jiang N, Wang D, Hu Z, Shin HJ, Qian G, Rahman MA, et al. Combination of anti-HER3 antibody MM-121/SAR256212 and cetuximab inhibits tumor growth in preclinical models of head and neck squamous cell carcinoma. *Mol Cancer Ther* 2014;13:1826–36.
- Wang D, Muller S, Amin AR, Huang D, Su L, Hu Z, et al. The pivotal role of integrin beta1 in metastasis of head and neck squamous cell carcinoma. *Clin Cancer Res* 2012;18:4589–99.
- D'Souza G, Carey TE, William WJr, Nguyen ML, Ko EC, Riddell J4th, et al. Epidemiology of head and neck squamous cell cancer among HIV-infected patients. *J Acquir Immune Defic Syndr* 2014;65:603–10.
- Schoeberl B, Faber AC, Li D, Liang MC, Crosby K, Onsum M, et al. An ErbB3 antibody, MM-121, is active in cancers with ligand-dependent activation. *Cancer Res* 2010;70:2485–94.
- Zhang H, Yun S, Batuwangala TD, Steward M, Holmes SD, Pan L, et al. A dual-targeting antibody against EGFR-VEGF for lung and head and neck cancer treatment. *Int J Cancer* 2012;131:956–69.
- Tzahar E, Waterman H, Chen X, Levkowitz G, Karunakaran D, Lavi S, et al. A hierarchical network of interreceptor interactions determines signal transduction by Neu differentiation factor/neuregulin and epidermal growth factor. *Mol Cell Biol* 1996;16:5276–87.
- Pinkas-Kramarski R, Soussan L, Waterman H, Levkowitz G, Alroy I, Klapper L, et al. Diversification of Neu differentiation factor and epidermal growth factor signaling by combinatorial receptor interactions. *EMBO J* 1996;15:2452–67.
- Holbro T, Beerli RR, Maurer F, Koziczak M, Barbas CFIII, Hynes NE. The ErbB2/ErbB3 heterodimer functions as an oncogenic unit: ErbB2 requires ErbB3 to drive breast tumor cell proliferation. *Proc Natl Acad Sci U S A* 2003;100:8933–8.
- Xia W, Lau YK, Zhang HZ, Xiao FY, Johnston DA, Liu AR, et al. Combination of EGFR, HER-2/neu, and HER-3 is a stronger predictor for the outcome of oral squamous cell carcinoma than any individual family members. *Clin Cancer Res* 1999;5:4164–74.
- Takikita M, Xie R, Chung JY, Cho H, Ylaja K, Hong SM, et al. Membranous expression of Her3 is associated with a decreased survival in head and neck squamous cell carcinoma. *J Transl Med* 2011;9:126.
- Bei R, Pompa G, Vitolo D, Moriconi E, Ciocci L, Quaranta M, et al. Colocalization of multiple ErbB receptors in stratified epithelium of oral squamous cell carcinoma. *J Pathol* 2001;195:343–8.
- Engelman JA, Zejnullahu K, Mitsudomi T, Song Y, Hyland C, Park JO, et al. MET amplification leads to gefitinib resistance in lung cancer by activating ERBB3 signaling. *Science* 2007;316:1039–43.
- Schaefer G, Haber L, Crocker LM, Shia S, Shao L, Dowbenko D, et al. A two-in-one antibody against HER3 and EGFR has superior inhibitory activity compared with monospecific antibodies. *Cancer Cell* 2011;20:472–86.
- Kawakami H, Okamoto I, Yonesaka K, Okamoto K, Shibata K, Shinkai Y, et al. The anti-HER3 antibody patritumab abrogates cetuximab resistance

- mediated by heregulin in colorectal cancer cells. *Oncotarget* 2014;5:11847–56.
38. Qian G, Jiang N, Wang D, Newman S, Kim S, Chen Z, et al. Heregulin and HER3 are prognostic biomarkers in oropharyngeal squamous cell carcinoma. *Cancer* 2015;121:3600–11.
  39. Citri A, Skaria KB, Yarden Y. The deaf and the dumb: the biology of ErbB-2 and ErbB-3. *Exp Cell Res* 2003;284:54–65.
  40. Chandralapaty S, Sawai A, Scaltriti M, Rodrik-Outmezguine V, Grbovic-Huezo O, Serra V, et al. AKT inhibition relieves feedback suppression of receptor tyrosine kinase expression and activity. *Cancer Cell* 2011;19:58–71.
  41. Huang S, Li C, Armstrong EA, Peet CR, Saker J, Amler LC, et al. Dual targeting of EGFR and HER3 with MEHD7945A overcomes acquired resistance to EGFR inhibitors and radiation. *Cancer Res* 2013;73:824–33.
  42. Shi F, Telesco SE, Liu Y, Radhakrishnan R, Lemmon MA. ErbB3/HER3 intracellular domain is competent to bind ATP and catalyze autophosphorylation. *Proc Natl Acad Sci U S A* 2010;107:7692–7.
  43. Vincenzi B. Hot topic: biology in anticancer treatment. *Curr Cancer Drug Targets* 2010;10:1–2.
  44. Ferris RL, Jaffee EM, Ferrone S. Tumor antigen-targeted, monoclonal antibody-based immunotherapy: clinical response, cellular immunity, and immunoescape. *J Clin Oncol* 2010;28:4390–9.
  45. Huang J, Wang S, Lyu H, Cai B, Yang X, Li F, et al. The anti-erbB3 antibody MM-121/SAR256212 in combination with trastuzumab exerts potent antitumor activity against trastuzumab-resistant breast cancer cells. *Mol Cancer* 2013;12:134.
  46. Tentler JJ, Tan AC, Weekes CD, Jimeno A, Leong S, Pitts TM, et al. Patient-derived tumour xenografts as models for oncology drug development. *Nat Rev Clin Oncol* 2012;9:338–50.
  47. Sanz L, Cuesta AM, Salas C, Corbacho C, Bellas C, Alvarez-Vallina L. Differential transplantability of human endothelial cells in colorectal cancer and renal cell carcinoma primary xenografts. *Lab Invest* 2009;89:91–7.
  48. Gray DR, Huss WJ, Yau JM, Durham LE, Werdin ES, Funkhouser WKJr, et al. Short-term human prostate primary xenografts: an in vivo model of human prostate cancer vasculature and angiogenesis. *Cancer Res* 2004;64:1712–21.
  49. Vandamme TF. Use of rodents as models of human diseases. *J Pharm Bioallied Sci* 2014;6:2–9.